Analytical Methods

COMMUNICATION

View Article Online
View Journal | View Issue

Published on 08 April 2016. Downloaded by University of Wisconsin-Milwaukee Libraries on 15/05/2017 22:22:08.

Cite this: *Anal. Methods*, 2016, **8**, 3440

Received 1st February 2016
Accepted 6th April 2016

DOI: 10.1039/c6ay00331a

www.rsc.org/methods

Label free nano-aptasensor for interleukin-6 in protein-dilute bio fluids such as sweat†

L. S. Selva Kumar,[a] Xiao Wang,[a] Joshua Hagen,[b] Rajesh Naik,[b] Ian Papautsky[a] and Jason Heikenfeld*[a]

A sub-pM limit of detection label-free sensor is presented for interleukin-6 based on impedimetric measurement of a gold nanoparticle/aptamer-modified electrode in artificial sweat.

Interleukin-6 (IL-6) is an important cytokine biomarker that is overexpressed in response to injury, inflammation and infection and the most prominent cytokine to appear in circulation during exercise.[1,2] In healthy individuals, IL-6 is present at a very low plasma concentration around 6 pg mL^{-1},[3] making the earlier diagnosis of diseases *via* detecting IL-6 a rather challenging task. IL-6 has also been shown to appear in eccrine sweat and have correlations with plasma levels,[4] which is a superior non-invasive access method compared to saliva which is confounded by inflammation of the gums and oral cavity. Some of the greatest value for sweat sensing[5,6] is the ability for wearable and/or continuous monitoring, which requires miniaturized sensor systems that are very simple to fabricate, operate, and which are compatible with commercial microcontrollers. However, sweat, like saliva, is ultra-filtered of protein content[7] such that protein content is orders of magnitudes lower than in blood.[8] Therefore very low detection limits are likely needed. Various immunological methods were developed for sensing IL-6 with a high sensitivity, selectivity and good detection limit.[9,10] But they are limited with antibodies synthesis, modification and denaturation.[11] A brief review of IL-6 sensors is provided in ESI.† These techniques highlighted require substantial time, machinery and specialist training. Compared to these technologies, the electrochemical method has been recognized as one of the most promising technologies because of its favorable portability, fast response, low cost, real-time detection, and environmentally-friendly nature. So, electrochemical impedance spectroscopy (EIS) based biosensors are well-suited to the detection of binding events happening in the transducer surface since minute changes in analytes to a biosensor surface can be easily and rapidly detected.[12] From a review of literature, no group has reported the electrical chemical detection of IL-6 using aptamers.

Aptamers are artificial functional oligonucleic acids selected *in vitro* through systematic evolution of ligands by exponential enrichment (SELEX) from random-sequence nucleic acids libraries.[13,14] Aptamers possess several advantages over antibodies, including smaller size, easier artificial synthesis and modification, and better stability. Furthermore, with a redox couple attached to the aptamer, surface fouling does not significantly change the electrochemical impedance.[15] Thus, the combination of EIS and IL-6 aptamer not only has excellent properties of an electrochemical technique but could also achieve high selectivity for IL-6 detection. At the same time, EIS-based aptasensors are label-free, overcoming complex and laborious process of labeling aptamers which might affect the bioaffinity between aptamers and their targets. Furthermore, for low-cost and wearable sweat sensors, label-free operation is highly attractive since it greatly reduces system complexity. Therefore, an EIS-based aptasensor is considered as an ideal choice for IL-6 detection in non-invasive biofluids such as sweat as shown in Scheme 1A and B.

In addition, to increase the amount of aptamer molecules anchored on electrode surface, metal nanoparticles can be immobilized on the substrate material.[16] Particularly, gold nanoparticles (AuNPs) show very attractive properties, such as favorable micro environment, good biocompatibility and high electron transferability. They have been widely used as the immobilization matrix in biosensors fabrication for enhancing biosensor performance.[17] In this work, the aptamers were functionalized with linker and co-adsorbents for maximizing IL-6 binding and specificity for aptamer-based self-assembled monolayers (SAMs) support on gold. To prevent nonspecific protein adsorption with aptamers on gold, coadsorbents incorporating oligo (ethylene oxide) units have been utilized.[18]

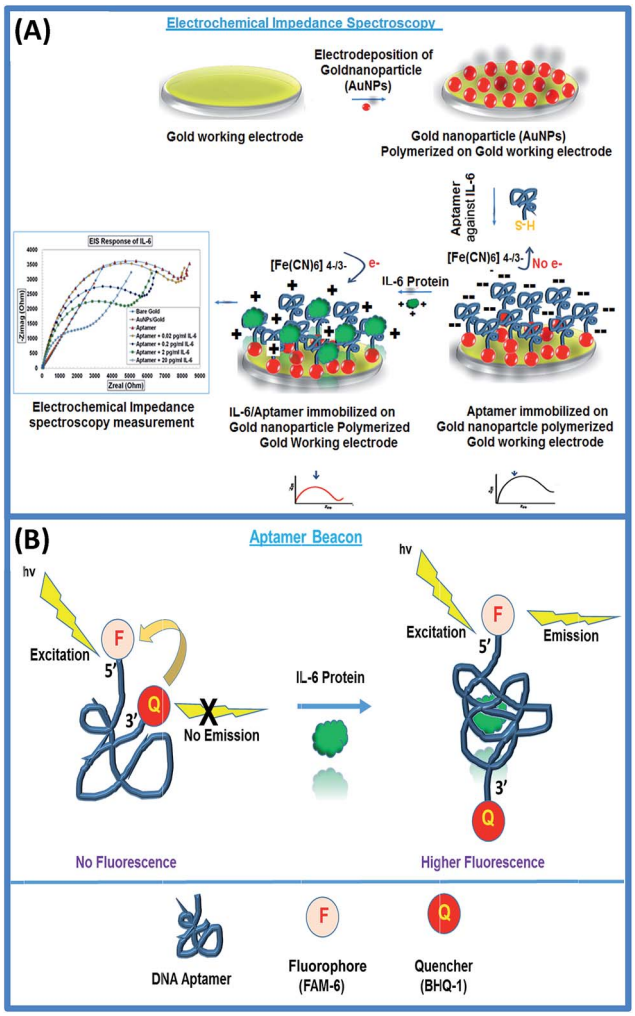
[a]*Dept. of Electrical Engineering and Computing Systems, University of Cincinnati, OH 45221, USA. E-mail: heikenjc@ucmail.uc.edu*

[b]*Air Force Research Laboratory, 711th Human Performance Wing, Wright Patterson AFB, OH 45433, USA*

† Electronic supplementary information (ESI) available: Detailed experimental procedures and supporting figures & tables. See DOI: 10.1039/c6ay00331a

This journal is © The Royal Society of Chemistry 2016

Published on 08 April 2016. Downloaded by University of Wisconsin-Milwaukee Libraries on 15/05/2017 22:22:08.



Scheme 1 (A) Schematic representation of the fabrication of the aptamer-based sensor and the experimental procedure followed for obtaining the analytical signal of IL-6 detection. (B) Scheme of the aptamer optical beacon assay for IL-6.

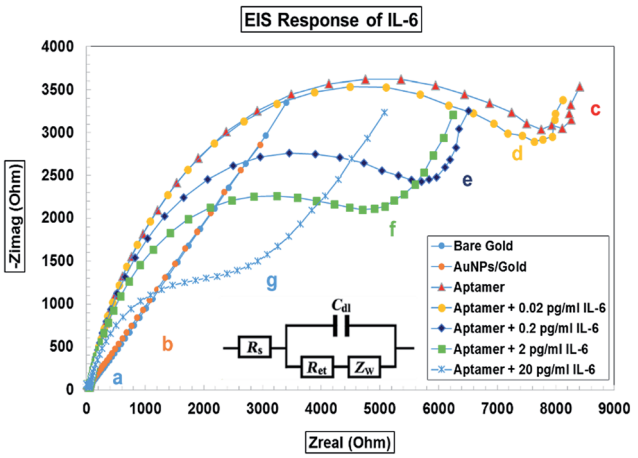


Fig. 1 Nyquist plots of impedance spectra obtained in 0.1 M PBS (pH 7.40) containing 5 mM $K_3Fe(CN)_6$ redox couple at (a) bare gold electrode; (b) AuNPs deposited on gold electrode; (c) 1 μM aptamer/AuNPs/gold electrode after interaction for 60 min; (d) 0.02 pg mL^{-1} of IL-6/1 μM aptamer/AuNPs/gold electrode; (e) 0.2 pg mL^{-1} of IL-6/1 μM aptamer/AuNPs/gold electrode; (f) 2 pg mL^{-1} of IL-6/1 μM aptamer/AuNPs/gold electrode; (g) 20 pg mL^{-1} of IL-6/1 μM aptamer/AuNPs/gold electrode; fitted data (solid line). The biased potential was 0.236 V. The frequency was from 1 MHz to 1.0 Hz and the amplitude was 5.0 mV. The inset shows the equivalent circuit applied to fit the impedance spectroscopy. The electrical equivalent circuit; R_s, R_{et}, Z_w and C_{dl} represent ohmic resistance of the electrolyte, electron transfer resistance, Warburg impedance and the double-layer capacitance, respectively.

The alkane thiol HS-$(CH_2)_{11}(OCH_2CH_2)_3OH$ (referred to as EG3) was chosen for this work as it is the shortest chain length of such coadsorbents reported to result in protein-resistant SAMs on gold.[19] Furthermore, currently EG3 has been used successfully when incorporated in DNA aptamer tethered SAMs.[20]

The electrochemical deposition of AuNPs on the surface of the gold electrode and cyclic voltammetry of the AuNPs/electrode surface is described in Fig. S1 and S2 (ESI†). In order to monitor each immobilization step and binding step, EIS and CV was performed in 0.1 M phosphate buffer containing 5 mM $K_3Fe(CN)_6$ (pH 7.4). The electrochemical impedance spectra, presented as Nyquist plots ($-Z_{im}$ *vs.* Z_{re}), of the gold working electrode and aptamer/AuNPs modified working electrode, are shown in Fig. 1. The bare working electrode showed a very small electron-transfer resistance (R_{et}, about 45 Ω), which was measured as the diameter of the semicircle in the Nyquist plot, suggesting a strong electron-transfer process at such electrode. A smaller semicircular region was observed at the AuNPs modified working electrode. The corresponding R_{et} value was estimated to be 33 Ω, which was significantly lower than that obtained for the bare working electrode. A bigger semicircular region was observed at the aptamer/AuNPs/modified working electrode. The corresponding R_{et} value was estimated to be 10.67×10^3 Ω, which was significantly larger than that obtained at the bare working electrode & AuNPs modified working electrode. Such behavior was mainly due to repulsive electrostatic interaction between the $Fe(CN)_6^{3-/4-}$ redox probe and negatively charged aptamer confined onto the gold electrode. The AuNPs can further enhance the electron transfer rate and improve the adsorption capacity of the electrode, and the AuNPs can increase the effective electrode surface area and thus have the potential to anchor more DNA aptamers to amplify the signal.

Fig. 1 also shows the Nyquist plots of the IL-6 aptamer based sensor after treatment with different concentrations of IL-6 protein. It can be observed that R_{et} value decreased with increasing concentration of IL-6 protein, implying a higher content of IL-6 protein captured onto the sensor surface. The R_{et} value was inversely proportional to the logarithmic value of IL-6 protein concentration over the range of 0.02 pg mL^{-1} to 20 pg mL^{-1}. It can be clearly observed that the electron-transfer resistance (semicircle diameter) decreases from 10.39×10^3 to 5.878×10^3 Ω as the protein concentration is elevated. Such drop in the R_{et} is consistent with the gradually increasing positive surface charge upon increasing the protein concentration, *i.e.*, growing electrostatic attraction of the electroactive marker. The detection limit (LOD) was calculated to be 0.02 pg

Published on 08 April 2016. Downloaded by University of Wisconsin-Milwaukee Libraries on 15/05/2017 22:22:08.

mL^{-1}, with regression coefficient of 0.9914, at which R_{et} was obtained when the sensor was incubated without IL-6 protein (Fig. 2). The limit of quantification (LOQ) is calculated as the concentration displaying a signal greater than the mean signal of the zero sample ($n = 5$). LOQ is 0.05 pg mL^{-1}. Please note that Fig. 2 is the relative change of charge transfer resistance ($\Delta R_{ct} = R_{ct} - R_{ct0}$), where R_{ct0} is the charge transfer resistance without IL-6 in a buffer and R_{ct} is the charge transfer resistance with a certain concentration of IL-6. However, after 20 pg mL^{-1} concentration the impedance values were not consistently decreasing due to saturation of IL-6 protein on the sensor surface (data not shown).

The results obtained from EIS are also in good agreement with the results obtained from the cyclic voltammograms (CV) characterization of the aptamer based biosensor in Fig. S3 (ESI†). When compared to CV, it was found that the change of the R_{et} in EIS was much more sensitive than the change of peak currents in cyclic voltammograms. Therefore, an EIS detection model is utilized in this work to obtain a high sensitivity.[21] Contrary to most impedance-based assays, we currently demonstrated that the aptamer–IL-6 protein interaction leads to a decrease (rather than the common increase) in the electron transfer resistance. As illustrated in Scheme 1, we speculate that the negatively-charged aptamer probe acts as an electrostatic barrier that repels the $Fe(CN)_6^{3-/4-}$ redox marker and hinders its interfacial electron transfer reaction; whereas the selective binding of the IL-6 protein to the aptamer-functionalized electrode provides an excess positive charge that facilitates transfer of the $Fe(CN)_6^{3-/4-}$ redox marker and therefore a stronger redox reaction. This is particularly useful, because it is likely the opposite of the effect of non-specific surface fouling of the sensor which could generally increase the impedance.

The inset of Fig. 1 shows the Randle modified equivalent circuit model used to fit the impedance spectroscopy and to determine electrical parameter values for each IL-6 concentration. As indicated from Table S1 (ESI†), the data validation carried out by the simplex test, proves that experimental results fit reasonably and are in a good agreement with the proposed circuit model. While the Z_w gives information about the diffusion of $Fe(CN)_6^{3-/4-}$ through the surface layer, the R_s values depend on the solution and the distance between working electrode and reference electrode. C models the capacitive behavior of the double layer replacing the infrequently ideal capacitance and diffusion behavior. However, the deviations from an ideal capacitance ($n = 1$) are reasonably small. On the other hand, the collected data after the aptamer–IL-6 protein interaction show that the values of R_{et} decrease significantly from 10.39×10^3 to 5.878×10^3 Ω upon increasing IL-6 concentration from 0.02 pg mL^{-1} to 20 pg mL^{-1} (Table S1) (ESI†), reflecting the less hindered charge transfer/marker diffusion. Very significant changes are observed for the C and W values.

EIS assay was validated with aptamer beacon assay as explained in effect of aptamer optimization on Beacon assay (ESI†). We observed a gradual increase in the fluorescence emission with a linear increase in the concentration of IL-6 as shown in Fig. S4 (ESI†). The detection was linear in the range 0.2 μg mL^{-1} to 200 μg mL^{-1} with a detection limit of 0.2 μg mL^{-1}. This brings to question, why the sensitivity is different for the aptamer in solution (optical beacon) *vs.* on a substrate (EIS). The reason for this enhancement of sensitivity is currently not known. However, similar phenomenon is observed for vasopressin & estrogen aptamers which exhibited a lower than expected sensitivity when applied to an EIS platform.[22,23] IL-6 is present in blood serum, a complex sample matrix, with hormones, lipids, blood cells and other proteins. Important to the purpose of this work, is measurement of IL-6 in sweat, in which it has been shown to correlate with protein ratios found in blood.[4] To study the selectivity of the system, we evaluated the response of different concentration of IL-6 added to commercial artificial sweat containing various amino acids,

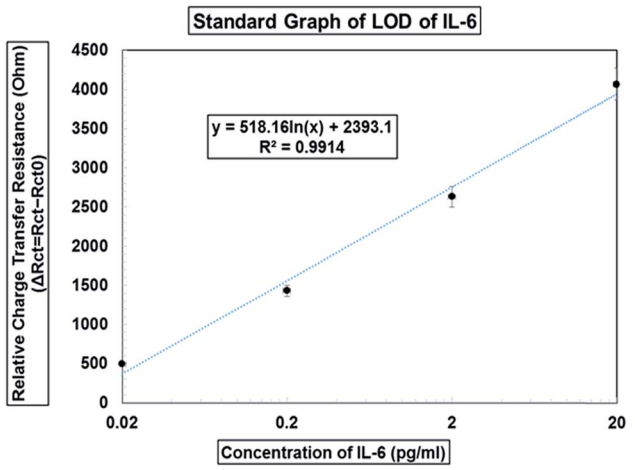


Fig. 2 EIS assay. Plot of relative charge transfer resistance ($\Delta R_{ct} = R_{ct} - R_{ct0}$) *versus* log of IL-6 concentration in pg mL^{-1}. Data were derived from quintuplets assays ($n = 5$) with error bars of 5%.

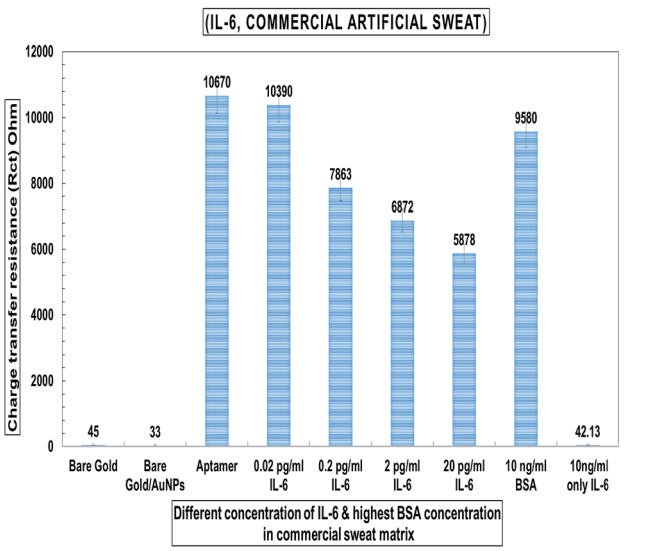


Fig. 3 Selectivity of IL-6 aptasensor. Plot of charge transfer resistance *versus* log of IL-6 concentration in pg mL^{-1} and highest concentration of albumin in commercial artificial sweat matrix. Data were derived from quintuplets assays ($n = 5$) with error bars of 5%.

 This journal is © The Royal Society of Chemistry 2016

Published on 08 April 2016. Downloaded by University of Wisconsin-Milwaukee Libraries on 15/05/2017 22:22:08.

Table 1 Results after commercial artificial sweat were spiked with IL-6 at four different concentration for precision studies using proposed method

	0.02 pg mL^{-1}	0.2 pg mL^{-1}	2 pg mL^{-1}	20 pg mL^{-1}
Replicate/day	5	5	5	5
Days	5	5	5	5
Mean	0.018	0.19	2.04	20.88
Standard deviation	0.002	0.02	0.19	0.90
Relative standard deviation (%)	14.1	10.6	9.55	4.32
Recovery (%)	90	97	102	104.4

metabolites & minerals as shown in Fig. 3. Respective Nyquist plots of impedimetric results in commercial artificial sweat are found in Fig. S5.† Artificial sweat mimics the real sweat environment like pH and salinity for validation of IL-6 sensor. In the first case, we tested albumin protein in highest concentration of 10 ng mL^{-1} in artificial sweat. When the sensor was incubated with BSA, there is slight decrease in electron interfacial resistance (shows less interferences).

Artificial sweat was then spiked with IL-6 at four different concentrations for precision studies as shown in Table 1. Each study was measured 5 times in duplicate on 5 different days. The rates of standard deviation were between 4.32% and 14.1% which is an acceptable range in precision studies. The stability of the aptasensor fabricated for the detection of IL-6 is also an important issue in practical applications. Therefore, the storage stability of the aptasensor was checked. After the aptasensor was stored in PBS (pH 7.4, 10 mM) at 4 °C in a refrigerator for over 2 weeks, the results showed 90% of original signal for the impedance response for the detection of 0.2 pg mL^{-1} IL-6. A plot of these results is provided in Fig. S6 (ESI†). We believe this shows that the sensor will be appropriate in real sweat. The detection limits and linear range for the IL-6 sensor demonstrated here are well below that required for use with blood. However, sweat, like saliva, is ultra-filtered of protein content[7] such that protein content is orders of magnitudes lower than in blood.[8] Therefore very low detection limits are likely needed, and this sensor may be ideal for use with ranges found in sweat. Further study is needed to determine ranges of IL-6 in sweat, and such studies should take into consideration possible IL-6 dilution at higher sweat rates.[24] The IL-6 sensor demonstrated in this work significantly de-risks the use of small-size and low-cost electronic methods for analysis of even pM biomarkers in sweat. Our group has recently reported small electronic patches, capable of measuring sweat nearly immediately as it emerges from the eccrine gland.[6] The IL-6 sensors of this work exhibit changes in resistance and use frequencies that are compatible with many small and low-power microcontroller chips that could be integrated into a sweat sensing patch. Furthermore, the use of a simple bulk-electrode technique is promising, as it does not require any micro or nanopatterning, and is therefore easier to integrate.

In conclusion, one final issue for the IL-6 sensor is that it is single use. A dissociation solution could be implemented to release the IL-6 to allow reuse, but could be complex to implement in an automatic microfluidic format. However, single-use may not be a major issue for sweat sensing for two reasons. Firstly, IL-6 over-expresses in response to most stimuli, so continuous monitoring could look simply for spikes in IL-6 concentration. Spikes in IL-6 would only increase the IL-6 bound at the sensor, such that upward trend in IL-6 could be measured at multiple times without need for disassociation of the IL-6. Second, fabricating one sensor has a cost similar to fabricating many with parallel microfabrication. So constructing multiple sensors and adding simple microfluidic gating could allow both up and down concentration trending measurements at hourly or other intervals.

Lastly, comparison to other approaches for IL-6 sensing is discussed. Several methods, to date, have been developed for the detection of IL-6 as shown in Table S2 (ESI†) such as enzyme-linked immunosorbent assay (ELISA), radioimmunoassay (RIA), conductometric immunoassay, electrochemical immunoassay, chemiluminescence assay, fluorescent microarray technology, surface enhanced Raman scattering (SERS) technology, *etc.* Despite many advances of these assays, some of them have drawbacks such as evident sample volume, complicated equipment, limited sensitivity, poor shelf life (stability), and clinically impractical time and expense. To show the advantages of our proposed sensor, a comparison table of the performances with different IL-6 aptasensors is shown in Table S2 (ESI†). From the Table S2 (ESI†), it can be seen that the LOD of our proposed sensor (0.02 pg mL^{-1}) is better than most analogous aptasensors and the linear range of our work is relatively wide. Future work will focus on: (1) improving the stability of aptamer in real sweat samples, such as chemical modification to enhance the nuclease resistance; (2) integration of the sensor into a fully functioning sweat collection and sensing patch.

Conflict of interest

Author Jason Heikenfeld discloses that he is a co-founder of Eccrine Systems Inc. which has commercial interest in sweat sensing technology.

Acknowledgements

This work was supported by funds provided by the Air Force Office of Scientific Research and by the Human Effectiveness Directorate, 711 Human Performance Wing, Air Force Research Laboratory. The Cincinnati authors would like to acknowledge support from an NSF (Eager Grant # 1347725), AFRL ORISE, and (NBMC grant # 14-008053-B00) for this work.

Notes and references

1 F. X. Bosch, J. Ribes, M. Diaz and R. Cleries, *Gastroenterology*, 2004, **127**, S5–S16.
2 J. Scheller and S. Rose-John, *Med. Microbiol. Immunol.*, 2006, **195**, 73–183.

Published on 08 April 2016. Downloaded by University of Wisconsin-Milwaukee Libraries on 15/05/2017 22:22:08.

3 C. B. Jacobs, M. J. Peairs and B. J. Venton, *Anal. Chim. Acta*, 2010, **662**, 105–127.
4 G. Cizza, H. M. Andrea, E. Farideh, C. C. Israel, T. Sara, N. S. Marni, M. P. Terry and E. M. Sternberg, *Biol. Psychiatry*, 2008, **64**, 907–911.
5 W. Jia, J. B. Amay, V. R. Gabriela, R. W. Joshua, Y. Zhanjun, R. Julian, C. Garrett and J. Wang, *Anal. Chem.*, 2013, **85**, 6553–6560.
6 D. P. Rose, M. Ratterman, D. K. Griffin, L. Hou, N. Kelley-Loughnane, R. R. Naik, J. A. Hagen, I. Papautsky and J. Heikenfeld, *IEEE Trans. Biomed. Eng.*, 2015, **62**, 1457–1465.
7 R. F. Vining and R. A. Mcginley, *J. Steroid Biochem.*, 1987, **27**, 81–94.
8 E. Csosz, G. Emri, G. Kall, G. Tsaprailis and J. Tozs, *J. Eur. Acad. Dermatol. Venereol.*, 2015, **29**, 2024–2031.
9 T. Li and M. H. Yang, *Sens. Actuators, B*, 2011, **158**, 361–365.
10 J. Peng, L. N. Feng, Z. J. Ren, L. P. Jiang and J. J. Zhu, *Small*, 2011, **20**, 2921–2928.
11 K.-M. Song, S. Lee and C. Ban, *Sensors*, 2012, **12**, 612–631.
12 A. E. Radi, J. L. A. Sanchez, E. Baldrich and C. K. O'Sullivan, *Anal. Chem.*, 2005, **77**, 6320–6323.
13 A. D. Ellington and J. W. Szostak, *Nature*, 1990, **346**, 818–822.
14 C. Tuerk and L. Gold, *Science*, 1990, **249**, 505–510.
15 A. L. Arica and K. W. Plaxco, *Acc. Chem. Res.*, 2010, **43**, 495–505.
16 S. Bamrungsap, T. Chen, M. I. Shukoor, Z. Chen, K. Sefah, Y. Chen and W. H. Tan, *ACS Nano*, 2012, **6**, 3974–3981.
17 Q. Huo, J. Colon, A. Cordero, J. Bogdanovic, C. Baker, S. Goodison and M. Pensky, *J. Nanobiotechnol.*, 2011, **9**, 1–12.
18 S. Balamurugan, A. Obubuafo, S. A. Soper, R. L. McCarley and D. A. Spivak, *Langmuir*, 2006, **22**, 6446–6453.
19 J. C. Love, L. A. Estroff, J. K. Kriebel, R. G. Nuzzo and G. M. Whitesides, *Chem. Rev.*, 2005, **105**, 1103–1169.
20 C. Boozer, J. Ladd, S. Chen, Q. Yu, J. Homola and S. Jiang, *Anal. Chem.*, 2004, **76**, 6967–6972.
21 X. Xia Li, L. Shen, D. Zhang, H. Qi, Q. Gao, F. Ma and C. Zhang, *Biosens. Bioelectron.*, 2008, **23**, 1624–1630.
22 B. J. Sanghavi, J. A. Moore, J. L. Chávez, J. A. Hagen, N. Kelley-Loughnane, C.-F. Chou and N. S. Swami, *Biosens. Bioelectron.*, 2016, **782**, 244–252.
23 Z. Lin, L. Chen, G. Zhang, Q. Liu, B. Qiu, Z. Caid and G. Chen, *Analyst*, 2012, **137**, 819–822.
24 Z. Sonner, E. Wilder, J. Heikenfeld, G. Kasting, F. Beyette, D. Swaile, F. Sherman, J. Joyce, J. Hagen, N. Kelley-Loughnane and R. R. Naik, *Biomicrofluidics*, 2015, **9**, 031301.

 This journal is © The Royal Society of Chemistry 2016